Statistical Analysis of the SNR Loss due to Imperfect Time Reversal

Guido Carlo Ferrante*†, Jocelyn Fiorina†, Maria-Gabriella Di Benedetto*

* Dept. of Information Engineering, Electronics and Telecommunications, Sapienza University of Rome, Rome, Italy
†Département de Télécommunications, Supélec, Gif-sur-Yvette, France

***Abstract*—Prefiltering, that is, linear processing at the transmitter side of a link, is often used in communication in order to simplify receivers, or to improve performance. Prefiltering requires at least a knowledge of the channel state. When this information is estimated, imperfect estimations impact achievable performance. Time reversal, that is a special kind of prefiltering, where channel is estimated at transmitter side during a training phase, is analyzed, in particular regarding the pattern of channel estimation errors. Results show that a loss in SNR is incurred, and a symbol error probability floor appears, depending on the variance of estimation errors. Exact theoretical expressions were derived for the SNR loss as well as symbol error probability.**

I. Introduction

Prefilters are introduced at the transmitter side of a communication system to simplify receivers, reduce the detrimental effect of several nuisance signals and distortions that the transmitted signal may be faced with, and improve performance. Typically, linear processing at the transmitter is also referred to as prefiltering and, similarly to linear processing at the receiver, may counteract noise only (transmit matched filter), interference only (transmit zero-forcing) or both noise and interference (transmit MMSE) [1], [2]. However, prefilters are derived under the assumption of perfect knowledge of the channel state, and other variables can be also required (*e.g.* the noise variance at the receiver in the case of transmit MMSE).

This paper investigates the effect of imperfect channel state information at the transmitter on the time reversal prefilter [3]–[5], also known as pre-Rake [6] or transmit matched filter [7], in terms of symbol error probability and SNR loss, as defined below, in a point-to-point ultra-wideband link.

The paper is organized as follows: Section II presents the model and the performance measures of interest; results are summarized in Section III, where a comparison with simulations is drawn. Theoretical derivations are collected in Appendix A. Conclusions are drawn in Section IV.

II. System Model

We consider a point-to-point link between two ultra-wideband transceivers, denoted by A and B, where information flows from A to B. The information-bearing signal of A depends on the channel between A and B, with impulse response denoted by $c(t)$, that is assumed reciprocal. This paper considers a time reversal prefilter, that allows to achieve, with a 1Rake, same performance as that achievable with an ARake. (The 1Rake reduces to a traditional receiver in absence of multipath.) To this end, both A and B require the knowledge of the channel. Transmission during a coherence time is, therefore, organized as follows (see, for example, [8], [9] for similar approach):

- **Training Phase I ($B \to A$):** B transmits a pseudonoise sequence and A correlates the received signal with the same known pseudonoise sequence, obtaining a noisy version of the channel impulse response (see, for example, [9]);
- **Training Phase II ($A \to B$):** B acquires the knowledge on the delay of the strongest path of the effective channel formed by the cascade of the time reversal prefilter and the multipath channel, for example by estimating the channel impulse response as in Training Phase I;
- **Data Transmission Phase:** A transmits a set of symbols to B through an information-bearing signal.

The first training phase is necessary to provide A with a knowledge of the channel impulse response. It will be used, once reversed in time, as the impulse response of the time reversal prefilter. This approach is usually adopted in several different contexts (*e.g.* , *naïve* precoding [10] or *mismatched* precoding [8], [11]). The second training phase is required in order to provide B with a knowledge of the *delay* of the strongest path. During this phase, B could estimate the whole channel impulse response: however, the delay of the strongest path is sufficient to set up the 1Rake receiver. Finally, during the data transmission phase, a sequential transmission of waveforms that modulate information-bearing symbols takes place. For the sake of simplicity, the basis pulse $\psi(t)$ that feds the time reversal prefilter is a zero-excess bandwidth waveform with band $[-W/2, W/2]$. An Additive White Gaussian Noise with variance σ_N^2 affects the received signal in the three phases.

In this paper, the channel state information at the transmitter (CSIT) is the impulse response of the multipath channel, and the channel state information at receiver (CSIR) is the delay of the strongest path of the channel impulse response, that is a very basic channel state information. According to the two-phase training described above, both CSIT and CSIR are imperfect. However, we assume hereinafter that CSIR is perfect, that is, the delay of the strongest path of the true channel impulse response is perfectly known.

978-1-4799-5396-7/14/$31.00 ©2014 IEEE

Based on the described training algorithm, samples of the channel estimated by A are:

$$\hat{\boldsymbol{c}} = \boldsymbol{c} + \boldsymbol{\xi} \;\in\; \mathbb{R}^{L+1}, \tag{1}$$

where L is the channel length in terms of samples ($L = T_d W$, being T_d the delay spread of the channel); $\boldsymbol{c} = [c_0, c_1, \ldots, c_L]^{\mathsf{T}}$ is the vector of samples of the channel impulse response, where:

$$c[i] = \langle\, c(t)\,,\, \psi(t - i/W)\,\rangle \triangleq \int_{-\infty}^{\infty} c(t)\psi(t - i/W)dt\ ;$$

$\boldsymbol{\xi} \sim \mathcal{N}(\boldsymbol{0}, \boldsymbol{I}\sigma_\xi^2)$ is a Gaussian random vector modeling the uncertainty of estimation, being $\sigma_\xi^2 = \sigma_N^2/\mathcal{E}_{\text{tr}}^{\text{r}}$ where $\mathcal{E}_{\text{tr}}^{\text{r}}$ is the energy of the training sequence received by A during the Training Phase I [9].

Focus on transmission of one symbol only, that for the sake of simplicity is assumed binary, $b \in \{-1, 1\}$. Assume that the symbol period is formed of N chips of duration $1/W$; therefore, the symbol period has duration $T_s = N/W$. The sampled received signal is:

$$\boldsymbol{y} = \sqrt{\mathcal{E}}\boldsymbol{C}\hat{\boldsymbol{p}}b + \boldsymbol{n},$$

where $\mathcal{E}$ is the trasmitted energy per symbol, $\boldsymbol{C}$ is the $(N + 2L) \times (N + L)$ convolution matrix describing the channel, $\hat{\boldsymbol{p}}$ is the $(N+L) \times 1$ transmitted waveform, and $\boldsymbol{n} \sim \mathcal{N}(\boldsymbol{0}, \sigma_N^2\boldsymbol{I})$. In particular, $\hat{p}[i] = \hat{c}[L-i]$ for $0 \le i \le L$, and $\hat{p}[i] = 0$ otherwise, where $\hat{c}[\ell]$ are the elements of $\hat{\boldsymbol{c}}$ as in eq. (1). A 1Rake yields to the following decision variable, upon which depends the decision on b:

$$\alpha = \sqrt{\mathcal{E}}\,\boldsymbol{c}^{\mathsf{T}}\frac{\boldsymbol{c} + \boldsymbol{\xi}}{\|\boldsymbol{c} + \boldsymbol{\xi}\|}b + n, \tag{2}$$

and $n \sim \mathcal{N}(0, \sigma_{\text{N}}^2)$. Define:

$$\zeta \triangleq \frac{\boldsymbol{c}^{\mathsf{T}}(\boldsymbol{c} + \boldsymbol{\xi})}{\|\boldsymbol{c}\| \cdot \|\boldsymbol{c} + \boldsymbol{\xi}\|}, \tag{3}$$

then eq. (2) becomes:

$$\alpha = \sqrt{\mathcal{E}}\,\|\boldsymbol{c}\|\,\zeta\, b + n. \tag{4}$$

The two performance measures analyzed are the signal-to-noise ratio SNR:

$$\mathsf{SNR} \triangleq \frac{\mathcal{E}\|\boldsymbol{c}\|^2\zeta^2}{\sigma_N^2}, \tag{5}$$

where ζ^2 is the SNR loss, that is a r.v. since $\boldsymbol{\xi}$ is a random vector, and the symbol error probability:

$$P_e = \mathbb{P}(\,\alpha < 0 \,|\, b = 1\,)\,. \tag{6}$$

III. Results

In this section, the pdf of ζ is discussed and its effect on SNR and P_e are explored.

As derived in Appendix A, the pdf of ζ is:

$$\mathsf{f}_\zeta(z) = \mathsf{f}_{\mathcal{T}'_L\left(\frac{\|\boldsymbol{c}\|}{\sigma_\xi}\right)}\left(\frac{\sqrt{L}}{\sqrt{1 - z^2}}z\right) \cdot \frac{\sqrt{L}}{\sqrt{(1 - z^2)^3}}\ ,\ |z| < 1\ , \tag{7}$$

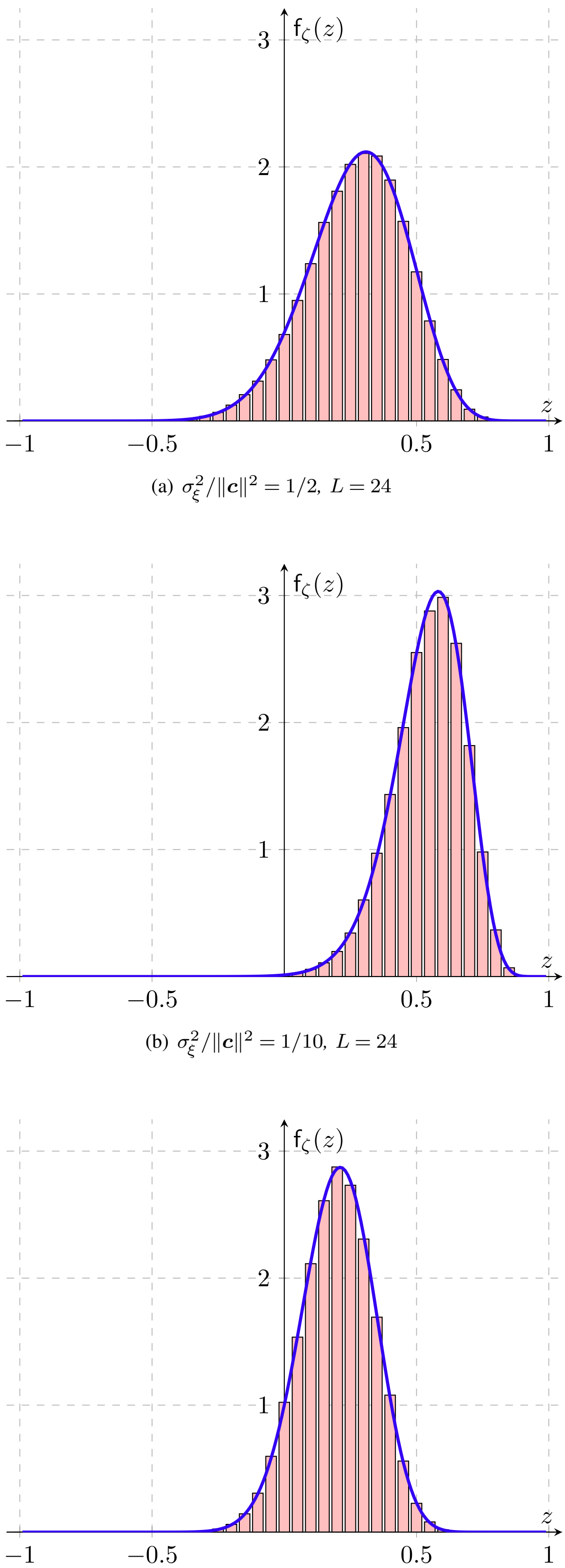

(a) $\sigma_\xi^2/\|\boldsymbol{c}\|^2 = 1/2,\ L = 24$

(b) $\sigma_\xi^2/\|\boldsymbol{c}\|^2 = 1/10,\ L = 24$

(c) $\sigma_\xi^2/\|\boldsymbol{c}\|^2 = 1/2,\ L = 48$

Fig. 1: Pdf of ζ: simulated histograms vs. theoretical expression of eq. (7). Parameters: L is the number of resolvable paths of the channel; σ_ξ^2 is the variance of the estimation error.

where $f_{\mathcal{T}'_L(\|\boldsymbol{c}\|/\sigma_\xi)}$ is the Student $\mathcal{T}$-distribution with L degrees of freedom and non-central parameter $\|\boldsymbol{c}\|/\sigma_\xi$. Figure 1 shows simulated histograms vs. $f_\zeta(z)$ for different values of L and $\sigma_\xi/\|\boldsymbol{c}\|$. Values of L corresponds, for example, to a channel with delay spread of $T_d \approx 50$ ns, and a signal with a bandwidth of $W \approx 0.5$ GHz. Values of $\sigma_\xi/\|\boldsymbol{c}\|$ depends on $\mathcal{E}^{\mathrm{r}}_{\mathrm{tr}}$, and, therefore, on the training sequence power and the duration of the training. By comparing Fig. 1(a) vs. (b), it is shown, as can be expected, that ζ approaches 1 when the estimation improves. It can be shown that, as $\sigma_\xi^2 \to 0$, *i.e.*, for vanishing estimation errors, the pdf tends to $\delta(z-1)$, and no loss in eq. (4) occurs. By comparing Fig. 1(a) vs. (c), it is shown that ζ departs from 1 as L increases. This can be intuitively justified as follows: for a given accuracy, the total uncertainty on the channel increases with the number of resolved paths $L = T_d W$, and, therefore, as L increases, the variance of the estimation error on each path must decrease to avoid reduced, or even worse, performance. Moreover, physical multipath channels become more and more sparse as bandwidth increases: the number of multipath components, that is, the number of resolvable paths, is indeed limited, and so is the energy gain that can be carried by the whole channel. Hence, as bandwidth increases, there are no multipath components in an increasing fraction of the L taps composing the resolved channel, that, therefore, become a mere source of nuisance.

Note that, in eq. (7), $\boldsymbol{c}$ is regarded as nonrandom since during each coherence time the channel remains constant. This allows to derive, for example, the symbol error probability that affects the system during a particular coherence time, as studied below. However, if average performance over multiple coherence time is of interest, then the pdf of ζ must be regarded as the conditional pdf given $\boldsymbol{c}$. Nonetheless, although ζ depends upon $\boldsymbol{c}$, f_ζ depends upon $\boldsymbol{c}$ only via $\|\boldsymbol{c}\|$. Not the entire channel realization affects ζ, but just its energy $\|\boldsymbol{c}\|^2$. Therefore, although in the following $\boldsymbol{c}$ is regarded as nonrandom, it is just $\|\boldsymbol{c}\|$ to be nonrandom, that is a fading coefficient.

There are two main detrimental effects that imperfect estimation implies on SNR and P_e.

The first effect is a reduction in the SNR. The variance of the useful term $\sqrt{\mathcal{E}}\|\boldsymbol{c}\|\zeta\, b$ in eq. (4) is, indeed, equal to $\mathcal{E}\|\boldsymbol{c}\|^2\zeta^2$: with perfect CSIT, $\zeta = 1$, while with imperfect CSIT, $\zeta \in [-1, 1)$, and therefore $\zeta^2 \in [0, 1)$ measures the loss of variance in the useful term, and thus in SNR (see eq. (5)), due to the imperfect knowledge of the channel.

The second effect is the presence of a symbol error probability floor depending on σ_ξ^2, irrespective of the amount of power spent in transmission (Data Transmission Phase), and only depending on the energy spent during the Training Phase I. Accuracy of estimation can bound, therefore, the achievability of low (uncoded) symbol error probability. The symbol error probability floor appears as $\mathcal{E}/\sigma_N^2 \to \infty$; in this asymptotic case, the decision variable tends to:

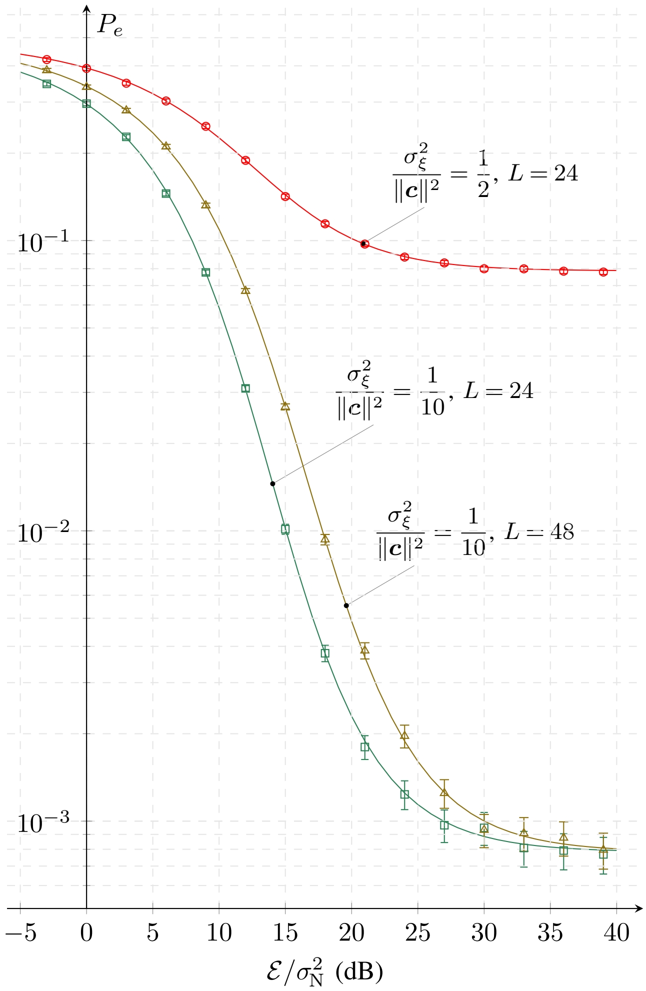

FIG. 2: Symbol error probability P_e vs. $\mathcal{E}/\sigma_N^2$ for different values of the number of resolved paths L and the estimation error variance σ_ξ^2.

$$\bar{\alpha} = \sqrt{\mathcal{E}}\,\frac{\boldsymbol{c}^{\mathsf{T}}(\boldsymbol{c}+\boldsymbol{\xi})}{\|\boldsymbol{c}+\boldsymbol{\xi}\|}b,$$

and decision on b is made based on the sign of $\bar{\alpha}$, hence:

$$\begin{aligned} P_e^{\text{floor}} &= \mathbb{P}(\,\bar{\alpha} < 0 \mid b = 1\,) \\ &= \mathbb{P}(\,\boldsymbol{c}^{\mathsf{T}}(\boldsymbol{c}+\boldsymbol{\xi}) < 0\,) = Q\left(\frac{\|\boldsymbol{c}\|}{\sigma_\xi}\right). \end{aligned}$$

The exact symbol error probability is (see eqs. (6) and (4)):

$$\begin{aligned} P_e &= \mathbb{P}(\,\alpha < 0 \mid b = 1\,) \\ &= \mathbb{P}(\sqrt{\mathcal{E}}\|\boldsymbol{c}\|\zeta + n < 0\,) \\ &= \int_{-1}^{1} dz\, Q\left(\frac{\sqrt{\mathcal{E}}\,\|\boldsymbol{c}\|\,z}{\sigma_N}\right) f_\zeta(z; L, \|\boldsymbol{c}\|/\sigma_\xi), \end{aligned} \tag{8}$$

where in $f_\zeta(z; L, \|\boldsymbol{c}\|/\sigma_\xi)$ it is made explicit the dependence on L and $\|\boldsymbol{c}\|/\sigma_\xi$ (see eq. (7)).

Figure 2 shows P_e vs. $\mathcal{E}/\sigma_N^2$ for different values of $\sigma_\xi^2/\|\boldsymbol{c}\|^2$ and L, and compares the symbol error rate obtained through

Monte-Carlo simulations (points with error bars on figure) with the analytical expression of P_e (solid lines) given by eq. (8). Observe that, as expected, increased accuracy of the estimation yields to decreased P_e^{floor}. Furthermore, for fixed σ_ξ^2 and $\mathcal{E}/\sigma_N^2$, increased L yields to increased P_e: increasing L by a factor of two implies a loss of approximately 3 dB for $P_e^{\text{floor}} \ll P_e \ll 1$ (see $5 \leq \mathcal{E}/\sigma_N^2 \leq 25$ dB on figure), while the floor does not depend on L, hence same performance is reached for high SNR irrespective of the bandwidth.

IV. Conclusions

This paper investigated the impact of channel estimation errors on the performance of a point-to-point link using time reversal at the transmitter and 1Rake at the receiver. Channel was estimated at both sides of the link during a training phase. Receiver was assumed to perfectly know the delay of the strongest path of the ideal channel. Instead, transmitter used the estimated channel impulse response: imperfection in the channel knowledge was modeled as additive and Gaussian due to the adopted training scheme. Performance were derived in terms of SNR and P_e, and showed that imperfect channel knowledge implies a loss in SNR and the appearance of a floor in P_e. Therefore, during a coherence time, the power spent for training bounds the minimum achievable P_e. Furthermore, results showed that, for a fixed P_e, increased bandwidth requires increased accuracy (lower σ_ξ^2).

Future work will focus on generalizing the above results on the coded regime (channel capacity), and to other prefiltering schemes, such as the transmit zero-forcing and transmit MMSE prefilters.

Appendix A
Derivation of the PDF of ζ and ζ^2

1) PDF of ζ.

An orthogonal transformation on $\boldsymbol{\xi}$ greatly simplifies the expression of ζ. We can think of $\boldsymbol{c}$ as the $(L+1)$-tuple of coordinates of a vector in $\mathbb{R}^{L+1}$ with respect to the canonical basis $\mathcal{B}$. A different orthonormal basis $\mathcal{B}'$ such that only the first coordinate of the vector is non-zero can be found, for example via the Gram-Schmidt orthogonalization. By denoting with $\boldsymbol{c}'$ the coordinates of the vector with respect to $\mathcal{B}'$, it results $\boldsymbol{c}' = (c_1', 0, \dots, 0)^\mathsf{T}$. For convenience, we choose the first vector of $\mathcal{B}'$ as $\boldsymbol{c}/\|\boldsymbol{c}\|$, hence $c_1' = \|\boldsymbol{c}\|$.

Call $\boldsymbol{Q}$ the matrix that changes coordinates from $\mathcal{B}$ to $\mathcal{B}'$; then $\boldsymbol{c}' = \boldsymbol{Q}\boldsymbol{c}$. It is a well-known result that $\boldsymbol{Q}$, that is the matrix that changes coordinates of vectors between two orthogonal bases, is an *orthogonal* matrix, *i.e.*, $\boldsymbol{Q}^{-1} = \boldsymbol{Q}^\mathsf{T}$. As a consequence, $\boldsymbol{Q}$ is also an *isometry*, that is, vectors transformed under the action of $\boldsymbol{Q}$ do not change their norm: $\|\boldsymbol{c}'\| = \|\boldsymbol{c}\|$.

We can rewrite ζ as follows:

$$\zeta = \frac{\boldsymbol{c}^\mathsf{T}(\boldsymbol{c}+\boldsymbol{\xi})}{\|\boldsymbol{c}\| \cdot \|\boldsymbol{c}+\boldsymbol{\xi}\|} = \frac{\boldsymbol{c}^\mathsf{T}\boldsymbol{Q}^\mathsf{T}\boldsymbol{Q}(\boldsymbol{c}+\boldsymbol{\xi})}{\|\boldsymbol{Q}\boldsymbol{c}\| \cdot \|\boldsymbol{Q}(\boldsymbol{c}+\boldsymbol{\xi})\|} = \frac{\boldsymbol{c}'^\mathsf{T}}{\|\boldsymbol{c}'\|} \cdot \frac{\boldsymbol{c}'+\boldsymbol{\xi}'}{\|\boldsymbol{c}'+\boldsymbol{\xi}'\|} = \frac{c_1'+\xi_1'}{\|\boldsymbol{c}'+\boldsymbol{\xi}'\|} \ .$$

Since $\boldsymbol{c}'/\|\boldsymbol{c}'\| = [1, 0, \dots, 0]^\mathsf{T}$, one has:

$$\|\boldsymbol{c}'+\boldsymbol{\xi}'\| = \sqrt{(c_1'+\xi_1')^2 + \xi_2'^2 + \cdots + \xi_{L+1}'^2} = \sqrt{(c_1'+\xi_1')^2 + \|\boldsymbol{\xi}'_{-1}\|^2} \ ,$$

where $\boldsymbol{\xi}'_{-1} \triangleq (\xi_2', \dots, \xi_{L+1}')^\mathsf{T}$, being $\{\xi_k' : k = 2, \dots, L+1\}$ a set of i.i.d. Gaussian r.vs. Define:

$$x \triangleq \frac{c_1'+\xi_1'}{\sigma_\xi} \sim \mathcal{N}(c_1'/\sigma_\xi, 1)$$

and:

$$y \triangleq \frac{\|\boldsymbol{\xi}'_{-1}\|}{\sigma_\xi} \sim \chi_L \ ;$$

hence ζ is as follows:

$$\zeta = \frac{x}{\sqrt{x^2+y^2}} = \frac{x/y}{\sqrt{1+(x/y)^2}}, \tag{9}$$

therefore ζ depends only on the ratio x/y. It is useful to define the following variable:

$$t \triangleq \frac{x}{\frac{1}{\sqrt{L}}y} \ ; \tag{10}$$

in fact, t is distributed according to a known distribution, that is the non-central Student $\mathcal{T}$-distribution with L degrees of freedom and non-central parameter $\sqrt{\lambda} \triangleq c_1'/\sigma_\xi = \|\boldsymbol{c}\|/\sigma_\xi$ [12], that we denote by $\mathcal{T}_L'(\sqrt{\lambda})$ and has the following canonical form:

$$\mathsf{f}_{\mathcal{T}_L'(\sqrt{\lambda})}(t) = \frac{2^L e^{-\frac{\lambda}{2}} L^{1+\frac{L}{2}}}{\pi(t^2+L)^{\frac{L+1}{2}}} \Gamma\left(\frac{L+1}{2}\right) H_{-1-L}\left(-\sqrt{\frac{\lambda}{2}}\frac{t}{\sqrt{t^2+L}}\right) \ ,$$

where $H_n(x)$ is the Hermite polynomial [12]. Then, since from eqs. (9) and (10), it results:

$$\zeta = \frac{t}{\sqrt{L+t^2}},$$

the pdf of ζ is obtained by a change of variables[1] as follows:

$$\mathsf{f}_\zeta(z) = \mathsf{f}_{\mathcal{T}_L'(\sqrt{\lambda})}\left(\frac{\sqrt{L}}{\sqrt{1-z^2}}z\right) \frac{\sqrt{L}}{\sqrt{(1-z^2)^3}} \ , \quad |z| \leq 1 \ .$$

2) PDF of ζ^2.

[1]The pdf of ζ can be obtained from that of t by guaranteeing that $|\mathsf{f}_{\mathcal{T}_L'(\sqrt{\lambda})}(t)dt| = |\mathsf{f}_\zeta(z)dz|$.

Write ζ^2 as follows:

$$\begin{aligned}\zeta^2 &= 1 - \frac{\|\boldsymbol{\xi}'_{-1}\|^2}{(c'_1+\xi'_1)^2 + \|\boldsymbol{\xi}'_{-1}\|^2} \\ &= 1 - \frac{1}{1 + \frac{(c'_1+\xi'_1)^2}{\|\boldsymbol{\xi}'_{-1}\|^2}} \\ &= 1 - \frac{1}{1 + \frac{1}{L}\frac{\left(\frac{c'_1}{\sigma_\xi}+\frac{\xi'_1}{\sigma_\xi}\right)^2}{\frac{1}{L}\left\|\frac{\boldsymbol{\xi}'_{-1}}{\sigma_\xi}\right\|^2}} = 1 - \frac{1}{1+\frac{1}{L}\frac{x^2}{y^2/L}} \\ &\qquad\qquad = 1 - \frac{1}{1+\frac{1}{L}\Psi},\end{aligned}$$

having defined $\Psi = \frac{x^2}{y^2/L}$. The pdf of ζ^2 can be traced back to a known distribution. In fact, since $x^2 \sim \chi'^2_1(c'^2_1/\sigma^2_\xi)$ and $y^2 \sim \chi^2_L$, ζ^2 depends on the ratio of two independent chi-square distributions. It is known as (non-central) $\mathcal{F}$ (ratio) *distribution* the pdf that describes the ratio of two independent chi-square distributions [12]. Precisely, if $X \sim \phi'^2_n(\lambda)$, $Y \sim \phi'^2_m(\eta)$, then $Z = \frac{X/n}{Y/m}$ has a *doubly non-central* $\mathcal{F}$ *ratio distribution* of orders (n, m) and non-centrality parameters (λ, η),

$$Z \sim \mathcal{F}'_{n,m}(\lambda, \eta).$$

In the present case, $n = 1$, $m = L$, $\lambda = c'^2_1/\sigma^2_\xi = \|\boldsymbol{c}\|^2/\sigma^2_\xi$ and $\eta = 0$, hence:

$$\Psi \sim \mathcal{F}'_{1,L}(c'^2_1/\sigma^2_\xi, 0).$$

Since:

$$\zeta^2 = 1 - \frac{1}{1+\frac{1}{L}\Psi},$$

the pdf ζ^2 can be derived from that of Ψ by a change of variables from Ψ to ζ^2, and assumes the following form:

$$\mathsf{f}_{\zeta^2}(x; L, \lambda) = \frac{e^{-\frac{\lambda}{2}}(1-x)^{\frac{L}{2}-1}}{\sqrt{x}B\left(\frac{1}{2},\frac{L}{2}\right)}\,{}_1F_1\left(\frac{L+1}{2};\frac{1}{2};\frac{\lambda}{2}x\right)\mathbb{1}_{[0,1]}(x),$$

where $B(\cdot,\cdot)$ is the Beta function and ${}_1F_1(\cdot;\cdot;\cdot)$ is the Kummer confluent hypergeometric function [12].

REFERENCES

[1] M. Joham, K. Kusume, M. H. Gzara, W. Utschick, and J. A. Nossek, "Transmit Wiener filter for the downlink of TDD DS-CDMA systems," in *Proc. IEEE 7th Int. Symp. Spread Spectr. Techn. and Appl. (ISSSTA)*, Prague, Czech Republic, 2002, pp. 9–13.

[2] D. P. Palomar and Y. Jiang, "MIMO transceiver design via majorization theory," *Found. Trends Commun. Inf. Theory*, vol. 3, no. 4, pp. 331–551, 2006.

[3] L. De Nardis, J. Fiorina, D. Panaitopol, and M.-G. Di Benedetto, "Combining UWB with time reversal for improved communication and positioning," *Telecommunication Systems*, vol. 52, no. 2, pp. 1145–1158, 2013.

[4] G. C. Ferrante, J. Fiorina, and M.-G. Di Benedetto, "Complexity reduction by combining time reversal and IR-UWB," in *Proc. IEEE Wireless Commun. and Networking Conf. (WCNC)*, Paris, France, 2012, pp. 28–31.

[5] A. E. Akogun, R. C. Qiu, and N. Guo, "Demonstrating time reversal in ultra-wideband communications using time domain measurements," in *Int. Instrumentation Symp.*, Knoxville, TN, USA, 2005, pp. 8–12.

[6] R. Esmailzadeh and M. Nakagawa, "Pre-rake diversity combination for direct sequence spread spectrum mobile communications systems," *IEICE Trans. Commun.*, vol. 76, no. 8, pp. 1008–1015, 1993.

[7] M. Joham, W. Utschick, and J. Nossek, "On the equivalence of prerake and transmit matched filter," in *Proc. 10th Aachen Symp. Signal Theory*, Aachen, Germany, 2001, pp. 313–318.

[8] B. Hassibi and B. Hochwald, "How much training is needed in multiple-antenna wireless links?" *IEEE Trans. Inf. Theory*, vol. 49, no. 4, pp. 951–963, 2003.

[9] E. Biglieri, *Coding for Wireless Channels*. New York: Springer-Verlag, 2005.

[10] G. Caire, N. Jindal, M. Kobayashi, and N. Ravindran, "Multiuser MIMO achievable rates with downlink training and channel state feedback," *IEEE Trans. Inf. Theory*, vol. 56, no. 6, pp. 2845–2866, 2010.

[11] N. Merhav, G. Kaplan, A. Lapidoth, and S. Shamai Shitz, "On information rates for mismatched decoders," *IEEE Trans. Inf. Theory*, vol. 40, no. 6, pp. 1953–1967, 1994.

[12] M. Abramowitz and I. A. Stegun, *Handbook of mathematical functions: with formulas, graphs, and mathematical tables*. New York: Dover Publications, 1964.